IN-PHANTOM OR IN-AIR DOSE IMAGING WITH SEPARATION OF THE DIFFERENT COMPONENTS

G. Gambarini

Department of Physics of the University and INFN, Milan, Italy

ABSTRACT

Imaging and profiling of the absorbed dose in air and in tissue-equivalent phantoms exposed to thermal neutrons were performed at the TAPIRO fast reactor (ENEA, Italy). The proposed methods, aimed at supporting the planning of Boron Neutron Capture Therapy (BNCT), allows measuring 3D distributions of the therapy dose not only in tumours, but also in normal tissue. Fricke-XylenolOrange-infused gel-dosimeters were designed, which allow imaging the absorbed dose by means of optical analysis, based on the detection of visible-light absorbance with a CCD camera. The various secondary radiation dose components can be separated through the differential analysis of dose images obtained with gels having different elemental compositions. In-phantom dose mapping was also performed with thermoluminescent dosimeters (TLD) and a method for separating different dose contributions was studied, based on different kinds of TLDs. The agreement of the results obtained with the two techniques confirmed the validity of the methods. Fluence measurements performed with activation techniques and Monte Carlo simulations have shown good consistency with the gel and TLD results, giving further support to confirm the reliability of the methods.

Introduction

For BNCT treatment planning, besides the therapy dose in tumour due to the reaction $^{10}B(n,\alpha)^{7}Li$, it is necessary to determine the dose delivered by thermal and epithermal neutrons in healthy tissue, because this dose determines the maximum neutron fluence admitted for treatments. Owing to the different linear energy transfer (LET) and relative biological effectiveness (RBE) of the various kinds of secondary radiation produced by neutron reactions in tissue, the determination of total dose is meaningless and the various contributions have to be separately identified.
The reactions mainly responsible of the released energy in tissue or tissue-equivalent materials are:

$$^{1}H(n,\gamma)^{2}H \qquad (\sigma = 0.33 \text{ b})$$

whose γ-rays (of 2.2 MeV) can travel many centimetres through tissue, and

$$^{14}N(n,p)^{14}C \qquad (\sigma = 1.81 \text{ b})$$

whose emitted protons (of about 0.6 MeV), have short range in tissue and give local dose deposition. Moreover, epithermal and fast neutrons undergo elastic scattering (mainly with hydrogen) so that recoil nuclei also contribute to the absorbed dose. The relative contributions to the total absorbed dose of the secondary radiation emitted in the above reported reactions change from point to point in the irradiated volume, and depend on the beam geometry, on the size and dimension of the irradiated volume and on the neutron energy spectrum.

The developed methods for in-phantom measuring the various components of the absorbed dose are based on gel-dosimeters and on thermoluminescence dosimeters (TLD).

Neutron source

Phantom irradiations were performed at the fast research reactor TAPIRO (ENEA, Casaccia, Rome) in the thermal and epithermal columns properly designed for BNCT experiments.

The thermal column consists in a graphite moderator (40 cm thick) containing a lead shield (13 cm thick) in order to shield reactor background. The irradiation volume, inside this structure, has cubic shape $18 \times 18 \times 18$ cm^3. The thermal neutron flux at the maximum reactor power in the center of the irradiation cavity has resulted to be nearly $5 \text{x } 10^{8}$ cm^{-2} s^{-1} and the average ã-dose-rate about $(9.3 \pm 1) \text{ x } 10^{-4}$ Gy s^{-1}. In Fig. 1, the thermal column during set up before phantom irradiation is shown.

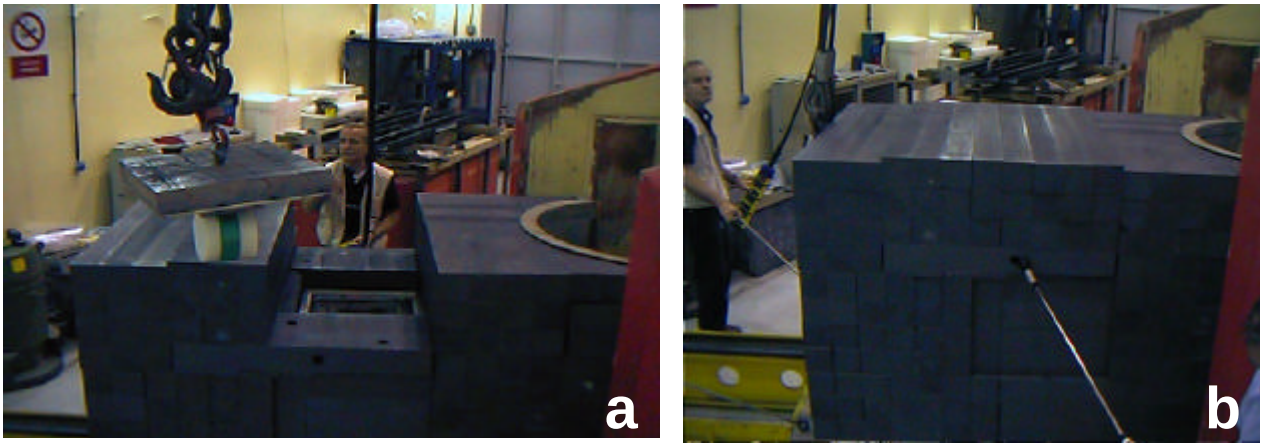

Fig. 1 – View of the thermal column during (a) phantom installation and (b) introduction in the reactor.

The epithermal column is a properly designed structure whose role is to shift the neutron spectrum towards epithermal energies. The irradiation volume is a parallelepiped-shaped chamber, 40x40 cm^2, and depth 70 cm. The collimator is squared, of 10x10 cm^2. During exposures, phantom are placed in front of the collimator mouth, supported by a very light wood structure. In Fig. 2, the irradiation volume is shown, (a) empty and (b) containing the phantom.

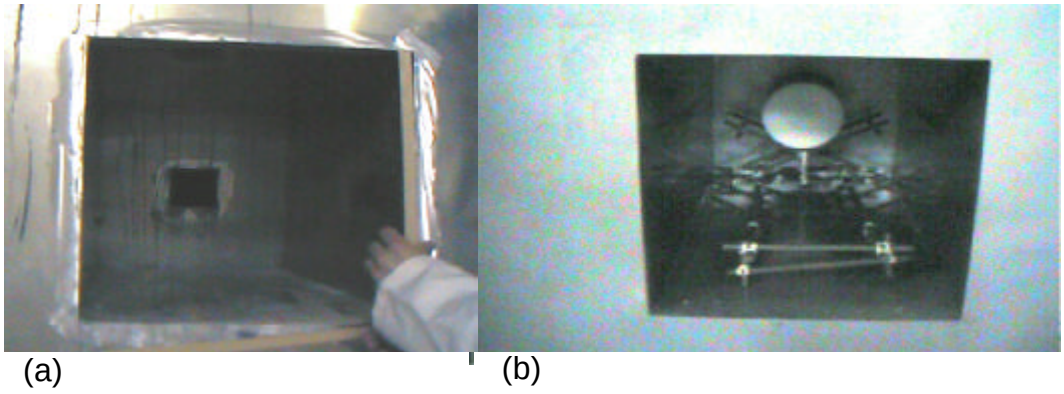

Fig. 2 - Irradiation volume of the epithermal column, (a) empty and (b) containing the phantom.

Gel dosimeters

Gel dosimeters consist in gel matrices in which a chemical dosimeters has been incorporated. This fact of being diluted water solutions makes gel dosimeters very promising for BNCT. In fact, like in human tissue, the action of ionising radiation starts with the radiolysis of water molecules and the solute, whose role is that of evincing the absorbed energy with a measurable effect, absorbs only negligible energy. This is true for every radiation field. In particular, in the case of neutron irradiations, each neutron-field component releases energy in a very similar way as in tissue. Moreover, by properly designing the isotopic composition of the gel matrix, the contributions to the absorbed dose can be suitably changed: then, the comparative analysis of results obtained with gels having different isotopic composition gives the possibility of separating the dose components.

Gel phantoms containing the same percentages of H and N as the tissue to be simulated and having the same density, have very good tissue-equivalence for neutrons: the energy is released exactly as in tissue of the same shape and volume of the phantom. The same gel, but depleted of N, absorbs all other dose components, but not the dose due to the protons emitted in the reaction with N. A gel added with the suitable amount of ^{10}B in the position of the tumour absorbs the previous doses plus

the therapy dose. It is easy to understand that proper manipulations of images detected from the various gel dosimeters allow separation of dose components. In fact, reliable results have been obtained introducing gel layers with suitable isotopic compositions in phantoms having good tissue-equivalence[1-3]. The separation of the fast neutron dose, mainly due to recoil-protons, is more difficult, because it comes from the same hydrogen nuclei that give γ-rays through interaction with thermal neutrons. The proposed method is based on comparison of the images detected with a tissue-equivalent gel and with a gel having the same composition, but made with heavy water. For achieving dose separation, preliminary calculation of the ratio between the energy released by protons and by deuterons in the two gel matrices is necessary. This ratio has been evaluated by means of Monte Carlo simulations [4,5].

In order to avoid perturbing the neutron transport in phantom and to maintain the reliability of measurements, only small gel volumes with different composition have been introduced. To this purpose, the suggestion is that of introducing, in tissue-equivalent phantoms, layers of dosimetry-gel where the doses have to been determined. In such a way, it is possible to have dose images or profiles in the plane were the dosimeter-layers have been introduced.

Gel-dosimeters have been obtained by incorporating Ferrous-sulphate and Xylenol-Orange in an Agarose-gel matrix. The effect of ionising radiation results in changes of visible-light absorption and the difference between the optical densities of absorbance images detected before and after exposure results to be proportional to the absorbed dose. As known, in ferrous sulphate solutions, chemical reactions occurring after exposure to ionising radiation give rise to oxidation of ferrous ions Fe^{++} to ferric ions Fe^{+++}, with ferric ion yield proportional to the absorbed dose, up to saturation effects. The metal ion indicator Xylenol Orange, induces optical absorption of visible light at about 450 nm and in presence of Fe^{+++} ions form a complex that gives absorption at about 585 nm. The difference in absorbance, at this last wavelength, between irradiated and non-irradiated gels has shown to be linearly correlated to the absorbed dose. Visually, the colour of the gel changes from orange to violet for increasing dose. In Fig. 3 (a,b), the apparatus for gel preparation is shown, near a photo of the operation of introducing with a syringe the hot Fricke-gel into the proper holders. In Fig. 3c, some irradiated dosimeters are shown. Transmittance images are detected utilizing a CCD camera[6]. The image manipulations, necessary in order to obtain quantitative dose images with good reliability, consist not only in application of the proper algorithms, characteristic of the utilized detection technique, but also in suitable normalization of the data obtained with gel-dosimeters having the various isotopic compositions. In fact, besides the difference in absorbed dose, the variation in gel composition can induce variation in sensitivity. Moreover, it is known that gel-dosimeter sensitivity depends on radiation LET. Then, each gel has different sensitivity to each secondary radiation produced by neutrons, that is to γ-rays, protons, electrons, α particles and so on. The sensitivity factor for α particles and lithium recoils, as resulted from experimental determination, is between 0.4 and 0.45[7]. For protons and deuterons, the sensitivity factor has been deduced by results found in literature, and the chosen values are 0.85 and 0.7 respectively.

Fig. 3 – The apparatus for gel dosimeter preparation (a), the final operation of performing gel samples (b) and some dosimeters irradiated at different ã-doses (c).

During these experiments, aimed at developing a method for measuring the absorbed doses in phantoms of interest for multiform glioblastoma treatments, the thickness of the employed gel layers was 3 mm. Lower thickness, up to 1 mm, has proved to give reliable results, but more care in sample preparation is necessary. In Fig.1, a gel layer, irradiated in a phantom exposed in the epithermal column of TAPIRO reactor, is shown. The sample is placed on the illuminator, near a strip of transmittance standards, with 10 different optical densities. The Grey Levels measured on the strip are utilized to test the stability of the light source and to evaluate eventual correction factors.

Fig. 4 - Gel dosimeter placed on the illuminator for detection of transmittance image.

TLDs

A method for dose profiling with thermoluminescent dosimeters (TLD) has been developed too. The method allows measurements of γ-dose and thermal neutron fluence. The proposed technique is based on the different responses to the different radiations of various kinds of TLDs and on the study of the Glow-Curve (GC) shapes. We used four kinds of TLDs (by Harshaw): TLD-300 (CaF_2:Tm), TLD-600 (LiF: Mg,Ti - 95.6% ^{6}Li), TLD-700 (LiF: Mg, Ti - 99.9% ^{7}Li) and TLD-100 (LiF: Mg, Ti - 7.5% ^{6}Li). The dosimeters have been placed inside the phantom in cavities of the same dimensions of the dosimeters themselves, as shown in Fig. 6, in order to avoid empty spaces.

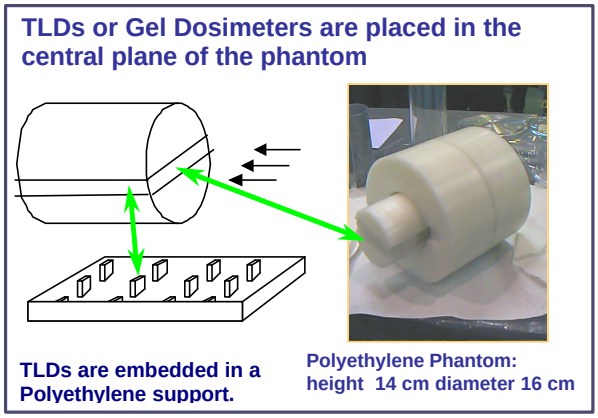

Fig. 6 – View of the polyethylene phantom and scheme of the dosemeter set up.

CaF_2 has been chosen for γ-dose measurements owing to its high sensitivity to gamma radiation and low sensitivity to slow neutrons. CaF_2 is produced with three kind of doping: CaF_2:Dy (TLD-200), CaF_2:Tm (TLD-300) and CaF_2:Mn (TLD-400). All such elements present not negligible cross sections for neutron capture and, as a consequence, the dosimeters undergoes internal β-irradiation. In the case of Dy (σ = 2700 barn, τ = 2.4 h) this effects gives a significant contribution to the dosimeter response, so that TLD-200 is not a good candidate for γ-dose measuring in BNCT. CaF_2:Mn and CaF_2:Tm seems to be more promising. In this work, only TLD-300 been studied, but TLD-400 too can be valid for the BNCT dosimetry[8]. CaF_2:Tm dosimeters (TLD-300), often employed for high-energy neutron dosimetry, show a sensitivity to neutrons that decreases with decreasing neutron energy and in the thermal or epithermal column of a nuclear reactor the neutron contribution has resulted to be negligible with respect to that of γ-radiation. This fact is confirmed by the constancy, within the experimental error, of the ratio of the low and high temperature peaks in the GCs of dosimeters exposed to ^{137}Cs γ-rays or to thermal and epithermal neutrons, since neutrons would produce an enhancement of the high temperature peaks. An example is shown in

Fig.7, where two GCs of a TLD-300 are reported, after irradiation with ^{137}Cs γ-rays and after exposure in phantom in the TAPIRO epithermal column.

The effect of self-irradiation has been studied, in order to investigate if the internal dose gives a sensible increase to the dosimeter response. Self-irradiation has resulted to be 10^2-10^3 times lower with respect to the dose to be measured, also in the case of multiple utilization of the dosimeters. The dependence of the TLD-300 response on photon energy has been investigated too. An increase of sensitivity for low photon energy has been found, with a maximum at about 45 keV. Notwithstanding this increase of response for low photon energies, TLD-300 has proved to give good results in dose measurements in the thermal or epithermal columns.

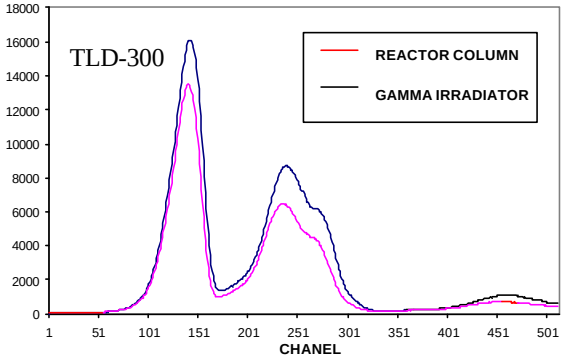

Fig. 7 – Glow curves of TLD-300 after exposure to ^{137}Cs γ-rays or in the TAPIRO main column.

LiF:Mg,Ti dosimeters are sensitive to both thermal neutrons and γ-rays, with relative contributions depending on the ^{6}Li and ^{7}Li percentage. In fact, thermal neutrons give the following reactions: ^{7}Li(n, γ)^{8}Li (σ = 0.033 b) and ^{6}Li(n, α)^{3}H (σ = 945 b). The short range of the α and tritium particles causes high sensitivity to thermal neutrons of dosimeters containing ^{6}Li. TLD-700 contains only a very low amount of ^{6}LiF; nevertheless, in high neutron fluxes as those of BNCT, both γ-rays and neutrons contribute to TLD-700 luminescence. Therefore, to obtain the γ-dose with such dosimeters it is necessary to subtract the thermal neutron contribution (measured for example by means of activation foils or calculated) from the total dosimeter response. An example of the GC of a TLD-700 irradiated in the epithermal column is shown in Fig. 8. On the opposite, in TLD-600 the γ-dose gives a negligible contribution with respect to thermal neutrons, and the fluence of such neutrons can be directly obtained without subtraction of the γ-contribution. However, TLD-600 need more attention when utilised in high fluxes of thermal or epithermal columns. When exposed to high fluences of thermal neutrons, LiF dosimeters loose linearity and undergo radiation damage[9-11]. Such effects starts after about 2×10^9 cm^{-2} for TLD-600 and about 6×10^9 cm^{-2} for TLD-100. Such fluences are not so high, at the flux levels of BNCT. TLD-700 shows radiation damage effects only for fluences over 10^{13} cm^{-2}. LiF:Mg,Cu,P dosimeters have shown radiation damage effects starting at lower neutron fluences then LiF:Mg,Ti dosimeters. ^{7}LiF:Mg,Cu,P is sometimes considered more useful for γ-dose measurements than ^{7}LiF:Mg,Ti because its relative sensitivity to thermal neutrons with respect to γ-rays is lower. However, also for ^{7}LiF:Mg,Cu,P dosimeters, the thermal contribution is not negligible and it has to be subtracted in order to obtain good dose evaluations. For all such reasons and for the difficulty of achieving result reproducibility, LiF:Mg,Cu,P dosimeters have not been considered in the present study of dosimetry aimed at BNCT.

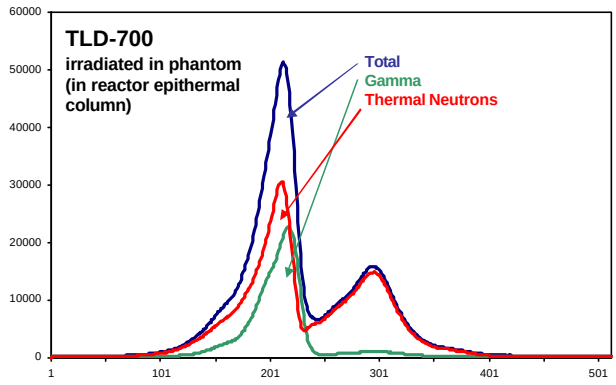

Fig. 8 - GC of a TLD-700 irradiated in the epithermal column, and separation of thermal-neutron and ã-ray contributions.

Self-irradiation effect is present in LiF dosimeters also, because the tritium generated in the ^{6}Li reaction is not stable (half-life 12.3 years) and a slow process of internal β irradiation gives a zero dose reading that depends on the neutron total fluence and on the time elapsed between dosimeter annealing and reading. This effect has resulted to be completely negligible if the dosimeters are re-utilized in high neutron fluxes. Obviously, after exposure to reactor neutron beams, dosimeters containing ^{6}Li have not to be utilised for personal dosimetry.

In conclusion, the method for ã-dose and thermal neutron fluence measurements with TLDs is:

1. The ã-dose is measured by means of TLD-300
2. The thermal neutron fluence is measured LiF:Mg,Ti dosimeters. If TLD-100 or TLD-700 are utilised, the ã-contribution is subtracted, on the basis of the ã-dose measured with a TLD-300 placed in the same position in the phantom and of the ã-calibration of the LiF dosimeter. For each dosimeter the ã-calibration has been performed, in order to reduce data dispersion. Further calibration controls have been performed too, in order to check the eventual effects of radiation damage. The thermal neutron calibration of the three TLD categories (TLD-600, TLD-100 and TLD-700) have been previously performed.

Results

Absorbed dose distributions have been measured in the central plane of a cylindrical phantom (14 cm of height and 16 cm of diameter) all made with polyethylene or made with a polyethylene cylindrical shell filled with gel containing 10 ppm of ^{10}B, both with and without a simulated tumour containing 35 ppm of ^{10}B. The absorbed dose in a phantom containing a volume with accumulation of 100 ppm of ^{157}Gd besides ^{10}B has been imaged too. In this case, to the composition of the gel around this tumour simulation, both 10 ppm of ^{10}B and 28.6 ppm of ^{157}Gd have been added. It is well known that in presence of ^{157}Gd, the thermal neutron capture reaction is highly probable:

$$^{157}Gd(n,\gamma)^{158}Gd \qquad (\sigma = 255000\ b)$$

and so, the γ-dose is sensibly increased in all the volume. Moreover, there is also production of internal-conversion and Auger electrons, and the electron dose has to be measures too, because radiobiological studies have revealed that such electrons present noticeable effects for cell killing.

In Fig 9, a sketch of the polyethylene phantom and a photo of one half of a phantom made with a shell filled with gel are show. Phantoms have been usually placed in the reactor columns with the cylinder axis fitting the beam axis. Only once the cylinder axis has been placed perpendicular to the beam axis, in order to enquire the difference in the dose and fluence profiles in the two cases.

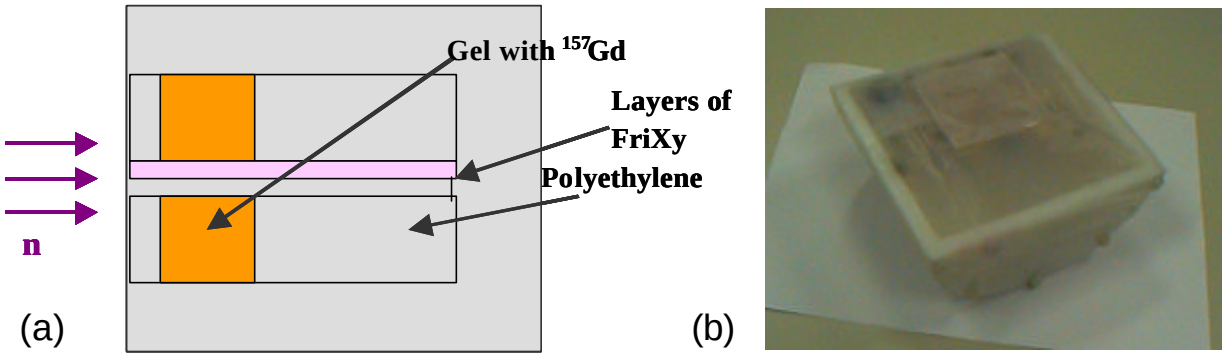

Fig. 9 - (a) Sketch of Polyethylene cylindrical phantom containing a simulated tumour (3 cm of height and 7 cm of diameter) and (b) view of one half of a phantom made of gel in a polyethylene shell and containing a simulated tumour.

In-air and in-phantom measurements have been performed with the above described methods. In-air measurements have been aimed at characterising the thermal and epithermal columns. In-phantom measurements were initially made with the purpose of inspecting the potentiality of the methods and finally to enquire the absorbed doses in some configurations of interest.

In Figs. 10-12 and in Tab. 1 some results obtained for the characterizations of the columns and in phantoms are reported.

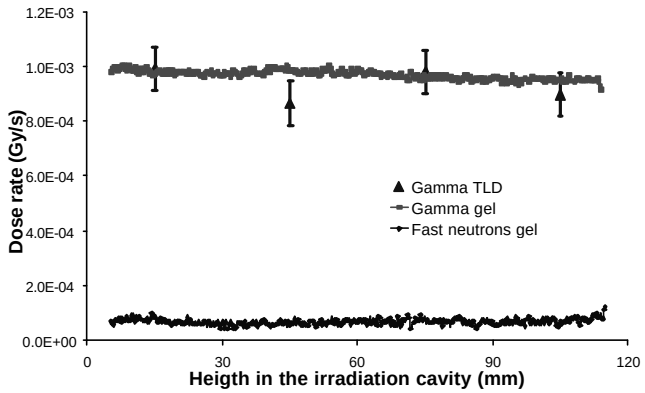

Fig. 12 - Gamma and fast neutron doses in the central region of the irradiation volume.

Fluxes	Monte Carlo	Experimental
Epithermal Neutrons	9.61×10^{8} (cm^{-2} s^{-1})	$7.45 \pm 0.15 \times 10^{8}$ (cm^{-2} s^{-1})
Thermal Neutrons	3.2×10^{7} (cm^{-2} s^{-1})	$1.30 \pm 0.20 \times 10^{7}$ (cm^{-2} s^{-1})
Dose / fluence		
D_{fast} / Φ_{epi}	5.38×10^{-13} ($Gy \cdot cm^{2}$)	$(5.06 \pm 0.76)\times 10^{-13}$ ($Gy \cdot cm^{2}$)
$D\gamma / \Phi_{epi}$	3.74×10^{-13} ($Gy \cdot cm^{2}$)	$(6.90 \pm 1.00)\times 10^{-13}$ ($Gy \cdot cm^{2}$)

Tab. 1 – Epithermal and thermal neutron fluxes at the collimator exit. Fast neutron and gamma doses per neutron fluence unit.

Fig. 11 – Dose profiles in the central axis of a phantom containing a simulation of tumour with ^{10}B (35 ppm).

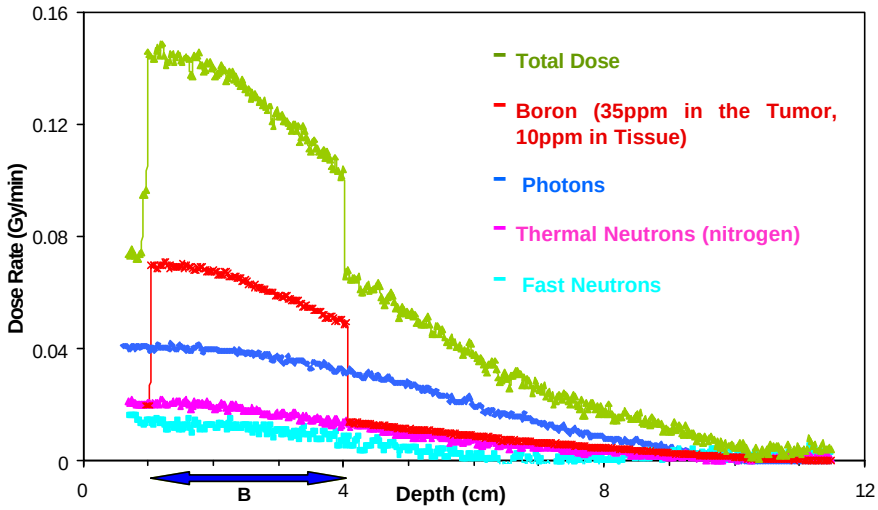

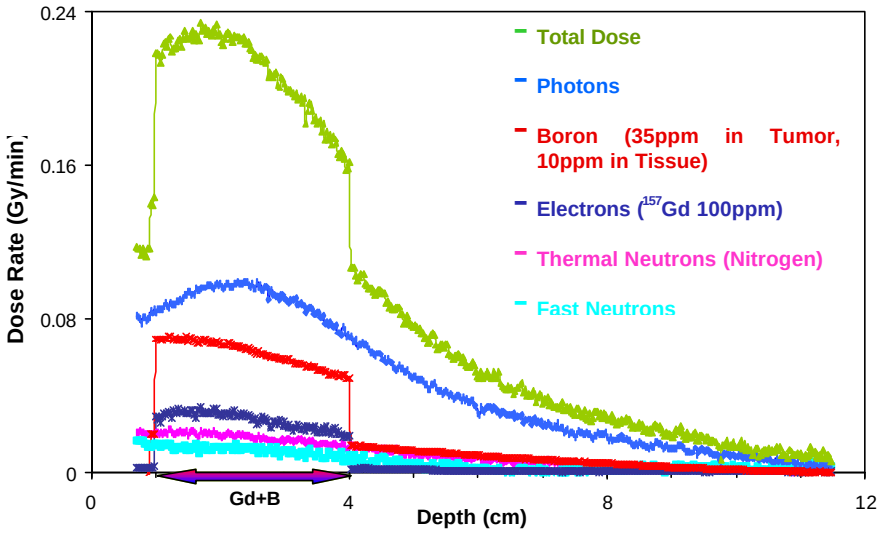

Fig. 12 – Dose profiles in the central axis of a phantom containing a simulation of tumour with ^{10}B (35 ppm) and ^{157}Gd (100 ppm).

Acknowledgments

The work was partially supported by INFN (Italy) and partially by MURST (Prot. 970916835_002 and Prot. 2001062789_002). Author is grateful to all the staff of the FriXy and TLD laboratory (Milan University, It) for the enthusiastic work on dosimeter preparation and analysis, and to the staff of TAPIRO reactor (ENEA, Casaccia, It), for the efficient collaboration during phantom exposures.

References

1. Gambarini, G., Birattari, C., Colombi, C., Pirola, L. and Rosi, G. - *Fricke-Gel Dosimetry in Boron Neutron Capture Therapy*. Radiat. Prot. Dosim. **101**, 419-422 (2002).
2. G. Gambarini, S. Agosteo, P. Marchesi, E. Nava, P. Palazzi, A. Pecci, R. Rosa, G. Rosi, R. Tinti. *Three-dimensional measurements of absorbed dose in BNCT by Frickee-gel imaging.* IAEA-TECDOC-**1223**, 152-164 (2001)
3. Gambarini, S. Agosteo, P. Marchesi, E. Nava, P. Palazzi, A. Pecci, G. Rosi, R.Tinti. *Discrimination of Various Contributions to the Absorbed Dose in BNCT: Fricke-Gel Imaging and Intercomaprison with other Experimental Results and Simulations.* Appl. Radiat. Isot. 53, 765-772 (2000)
4. G.Gambarini, S.Agosteo, U.Danesi,, F.Garbellini, B.Lietti, M.Mauri, G.Rosi. *Imaging and Profiling of Absorbed Dose in Neutron Capture Therapy*. IEEE Transactions on Nuclear Science, **48**, 780-784 (2001)G.
5. G.Gambarini, S.Agosteo, C.Colombi, O.Fiorani, B.Lietti, A.Perrone, P.Prestini, A.Riva, G.Rosi - *In-Phantom Measurements of 3-D Distribution of Dose-Components in Neutron Capture Therapy*. - in " Research and Development in Neutron Capture Therapy", W.Sauerwein R.Moss and A.Wittig eds., Monduzzi (Bologna, Italy) 2002, pp. 471-475
6. G.Gambarini, G.Gomarasca, A.Pecci, L.Pirola, R.Marchesini, S.Tomatis. *Three-dimensional determination of absorbed dose by spectrophotometric analysis of ferrous-sulphate agarose gel*. Nucl. Instr. and Meth. **A 422**, 643-648 , 1999.
7. V.Colli, C.Colombi, S.Gay, P.Prestini and L.Scolari. *In-Phantom Discrimination of the dose ciontributions by means of FriXy-Gel and Thermoluminescent dosemeters.* 3rd YOUNG members Neutron Capture Therapy Meeting, Pisa, Italy, 28 November (2003)
8. S.W.Martsolf, J.E.Johnson, C.E.D.Vostmyer, B.D.Albertson and S.E.Binney. *Practical Considerations for TLD-400/700-Based Gamma Ray Dosimetry for BNCT Applications in a High Thermal Neutron Fluence.* Health Phys. **69**, 966-970 (1995).
9. Ayyangar, K., Lakshmanan, A. R., Bhuwan Chandra and K.Ramadas, K. *A Comparison of Thermal Neutron and Gamma Ray Sensitivities of Common TLD Materials.* Phys. Med. Biol., **19**, 665-676 (1974).
10. Piesch E., Burgkhardt B. and Sayed A.M. *Activation and Damage Effects in TLD600 after Neutron Irradiation.* Nucl. Instr. and Meth. **157,** 179-184 (1978).
11. G.Gambarini, M. Martini, A. Scacco, C. Raffaglio, A.E. Sichirollo - *TL Dosimetry in High Fluxes of Thermal Neutrons Using Variously Doped LiF and $KMgF_3$.* Radiat. Prot. Dosim., **70**, 175-180 (1997).